

Flexural Creep Behavior in Utilization of Woven Glass-Fibre as Reinforcement in Pultruded Glass Fibre-Reinforced Polymer Composite Cross-Arms: Experimental and Numerical Analysis

A.L. Amir^{1*}, S. Yamunan¹, M.R. Ishak^{1,2,3}, N. Yidris¹ and M.Y.M. Zuhri⁴

¹Department of Aerospace Engineering, Universiti Putra Malaysia, 43400 UPM Serdang, Selangor, Malaysia

²Aerospace Malaysia Research Centre (AMRC), Universiti Putra Malaysia, 43400 UPM Serdang, Selangor, Malaysia

³Laboratory of Biocomposite Technology, Institute of Tropical Forestry and Forest Products (INTROP), Universiti Putra Malaysia, 43400 UPM Serdang, Selangor, Malaysia

⁴Advanced Engineering Materials and Composites Research Centre (AEMC), Department of Mechanical and Manufacturing Engineering, Universiti Putra Malaysia, 43400 UPM Serdang, Selangor, Malaysia

Abstract. Pultruded glass fiber-reinforced polymer (PGFRP) composite is a relatively new material used to replace conventional wood in the fabrication of cross-arms for transmission towers. Much research has been undertaken on coupon-scale PGFRP composite cross-arms. However, a few have been completed on full-scale PGFRP composite cross-arms under actual operating load. Thus, this work investigates the effect of wrapping woven glass fiber fabric as an additional reinforcement on the creep reactions of PGFRP composite cross-arms installed in a 132 kV transmission tower. In the first stage of this research, the deflection of the original cross-arm under various loads ranging from 0 to 9 kN was evaluated and was followed by the actual working loads. This experiment was repeated on cross-arms wrapped with different numbers of glass fiber fabric layers around the weakest point of the beam. Then, the creep behaviors and responses of the woven glass fiber-reinforced cross-arms were evaluated and compared with the original cross-arms from the previous study. The actual operating load was applied to the PGFRP composite cross-arms for 1000 hours to study their capability to support the weight of electrical cables and insulators. In order to replicate the tropical climate, the cross-arm were mounted on a test rig in an open area. The findings of this study revealed that reinforcing the cross-arm by wrapping it with woven glass fiber fabric could extend its life and hence reduce the maintenance cost and effort for long-term usage. The finding of this study will also become essential knowledge on woven fabric wrapping applications on square profiles.

* amirabdlatif786@gmail.com

1 Introduction

The transmission towers are used to carry transmission lines that connect power generators to substations as practiced in electrical power systems. Transmission towers are classified as latticed steel towers or monopole steel tubes. Steel lattice towers have been constructed throughout Peninsular Malaysia since 1929 to transmit electricity to residential and industrial sectors [1,2]. These towers comprise a peak, a cage, a tower body, a beam, and a cross-arms. Cross-arms secure utility wires and their insulators to the tower and ensure that the wires are at a safe distance above the ground. In former times, wooden cross-arms made from Chengal wood (*Neobalanocarpus heimii*) were used due to their excellent mechanical performance and arc-quenching properties after lightning strikes. Due to the growth of natural wood flaws over time and the scarcity of Chengal timber, cross-arms made from pultruded glass fiber-reinforced polymer composite (PGFRPC) are seen as an alternative to wooden cross-arms [3]. The first pilot project, in which PGFRPC cross-arms were installed on a 132 kV transmission tower in Pekan Town's Tanjung Batu line, was launched in 1999 [4,5]. Composites made of fiber-reinforced polymers have found application in various industries and are frequently used in the fabrication of automotive components, fire extinguishers, and household items due to their high stiffness and mechanical strength [6–9]. To investigate the mechanical performance of PGFRPC cross-arm assemblies and compile technical information on the impact of material qualities on structural integrity, numerous research investigations integrating computational modelling have been carried out. The impact of static load and sleeve placement has also been examined using computational simulation analyses of PGFRPC cross-arms [10–12] and the stacking sequence of fiber laminate on cross-arm assemblies, the impact of cross-arm failure due to laminate properties under multiaxial load [13–15], and the effect of material configuration of composite cross-arm by considering the static deformation [16]. Mechanical testing on the construction of creep test rigs for cross-arms has also been undertaken over an extended period. Despite various numerical models and test rigs, there is a dearth of research for PGFRPC cross-arms especially on the creep behaviors.

Several researchers have reported on the experimental and theoretical deflection of structural members of an initially-straight cantilever beam subjected to a specific load. Numerous examples of such cases call for the study of small and large deflection behavior of cantilever beams, such as folder-locking mechanisms, window-locking mechanisms, pole vaults, board jumps, and fishing rods. Singhal et al. [17] developed a theoretical solution for small and large deflection analysis of cantilever beams. The transverse or vertical deflection of the cantilever member's tip is linear in the small deflection theory. The tip's longitudinal or horizontal deflection, on the other hand, is inconsequential. While the large deflection analysis forecasts transverse and longitudinal deflections that are both realistic and nonlinear. In the linear elastic working range, however, both small and large deflection procedures provide the identical outcomes, therefore one can use the straightforward small deflection strategy for engineering design [18,19]. Moreover, the small deflection behavior analysis establishes the basic requirement for structural design and identifies the extent of the structure's applicability. Generally, the Bernoulli-Euler theory and the fundamental Hooke's law are used to analyze beam bending behavior [20–22]. The Bernoulli-Euler theory states that the bending moment at any point on a beam is proportional to the corresponding curvature, while Hooke's law states that the applied load is proportional to the extension as long as the deflection is small and the beam material does not yield.

In civil infrastructure, construction, and maritime applications, polymer matrix composites are gaining appeal as an alternative to traditional materials such as steel, wood,

and metals due to their high mechanical strength, low density, and superior corrosion resistance. Their variety and uncomplicated production makethem the preferred material for technical applications [23]. Glass fiber, particularly, is a lightweight, durable, and strong material. Compared to other composites, glass fiber-reinforced composites have a wide technical basis and extensive service experience. Thus, they are regarded as the most reliable engineering materials. Various composite qualities can be achieved by weaving the fibers in various patterns. Woven fabric composites are finding more and more applications in aircraft, vehicle constructions, and superconducting magnet equipment due to their distinctive architectural characteristics, simplicity of handling, low manufacturing cost, and exceptional mechanical qualities [24]. Nevertheless, an accurate and repeatable quantitative characterization of the composite's physical properties, particularly the mechanical qualities is quite challenging. This presents a unique problem, typically for the fiber-reinforced polymercomposites as they are one to four times stronger and stiffer than their empty matrices.

Compressive and tensile reactions of glass fiber-reinforced polymer composites, mainly woven glass fiber-reinforced polymer composites, have been extensively investigated. Several factors influence the compressive and tensile behavior of woven glass fiber-reinforced polymer composite materials, such as the type of material, weaving pattern, fabric geometry, fiber volume fraction, laminate configuration [25], void content, and woven linear density. On top of these factors, the fiber and matrix mechanical properties are the most influential. Zhong Xiang et al. studied the importance of interlayer friction in producing woven glass fiber fabric rolls. They also introduced the woven fabric to a commercial fabric winding machine to verify the effectiveness of the proposed method in improving winding quality [26]. The results revealed that the suggested rolling tension should be enforced at the inflection point of the fabric winding at a certain rolling velocity. V.A.Nelyub has discussed different methods of production of large-scale articles from polymer composite materials and found that the use of suit materials and best technological solutions in the winding method provides a required quality in electric transmission lines [27] produced an orthogonal net-shaped continuous structure using circular woven fabric via the hand lay-up method, in which the fabric was wet with epoxy. It was proven that the manual laying method has moderate estimated productivity and low stability. Nonetheless, the cost of this method is lower compared to others [28]. The circular woven preform provides a seamless continuous reinforcement for composite pipes with no starting and ending points. Several studies have shown that winding and hand lay-up of woven composites can improve the performance of structures and parts. However, studies on the use of the wrapping technique to produce square profile beams from woven composites are still lacking.

The creep phenomenon is mechanically occurs when a material is subjected to long-term steady stress. This deformation begins with instantaneous deformation and leads to structural failure after going through primary (transient), secondary (steady-state), and tertiary (accelerated) deformations. During the primary creep stage, the creep rate reduces linearly with passing time as a result of strain hardening or moveable dislocations. As a balance between the rates of dislocation production and recovery is reached during the secondary creep stage, the creep rate is almost constant. A rapid increase in creep rate follows the tertiary creep stage until the material ruptures due to the overall strain applied over time. The shear yielding in creep results, void chain slippage, growth development and fiber breakage over time. These occurrences cause the material to fracture. The current composite cross-arms are thought of as anisotropic structures since they are pultruded from an E-glass fiber-reinforced unsaturated polyester composite. Due to the induced creep rupture, this composite material occasionally displays interfacial strength instability, which reduces the mechanical

strength of the material structure.

Creep tests performed on composite cross-arms are necessary to codify, analyze extensively, and forecast creep tendencies over long-term service. To improve the long-term durability of PGFRPC cross-arms, this study compares and evaluates their long-term mechanical performance with the current cross-arms utilized in 132 kV transmission towers. By conducting a creep test on a full-size cross-arm under real load in a tropical environment, crucial data may be gathered and analysed. This strategy will help in accumulating information and predicting the long-term mechanical durability of the current cross-arm systems strengthened with composite. It will also offer an intuitive and incredibly thorough lens through which to view the behaviour of the entire system. In latticed transmission towers, PGFRPC cross-arms have only lately taken the place of conventional hardwood cross-arms. The creep behaviour of full-scale PGFRPC cross-arms in 132 kV transmission towers has thus received little attention in the literature. The purpose of this study is to ascertain the impact of reinforcing using the manual woven composite winding method on the performance and creep behaviours of PGFRPC cross-arms in transmission towers under actual stress condition. Additionally, the creep properties of the full-scale PGFRPC cross-arms are to be characterized. The findings of this study are expected to give academicians and engineers a practical viewpoint on the long-term mechanical behavior and a life prediction of PGFRPC cross-arms.

2 Methodology

The experimental works involved analyzing and evaluating the properties of PGFRPC cross-arms installed on high transmission towers in Malaysia. This chapter discusses the process of wrapping woven fabric to reinforce PGFRPC cross-arms. A two-stage methodology was employed in this research: experimental and data analyses. The following sub-sections cover the techniques and steps involved in detail.

2.1 Material Preparation

The main test subject of this research is the 132 kV PGFRPC cross-arm used for a suspension tower in Malaysia. The cross-arm was purchased from Electrius Sdn Bhd in Selangor, Malaysia, a regional producer of cross-arms. One tie and two main members, which made up the entire cross-arm assembly, were made using the pultrusion method with E-glass as the reinforcement fibre and unsaturated polyester resin as the matrix. The dimension of the square section of the cross-arm was $102 \times 102 \text{ mm}^2$ and had a fine, homogenous, and unidirectional fiber texture along the direction of the polymer matrix composites, which in accordance with the specification stated in Tenaga Nasional Berhad (TNB) standard. The tie member was 3472 mm long, whereas the length of the main cross-arm members was 3651 mm. Each cross-arm member was fastened to the test rig with bolts, nuts, and fastening brackets. A load was applied at the free end of the cross-arm, following the TNB standard of workload in actual condition. Figure 1 shows the complete schematic and actual view of the cross-arm assembly.

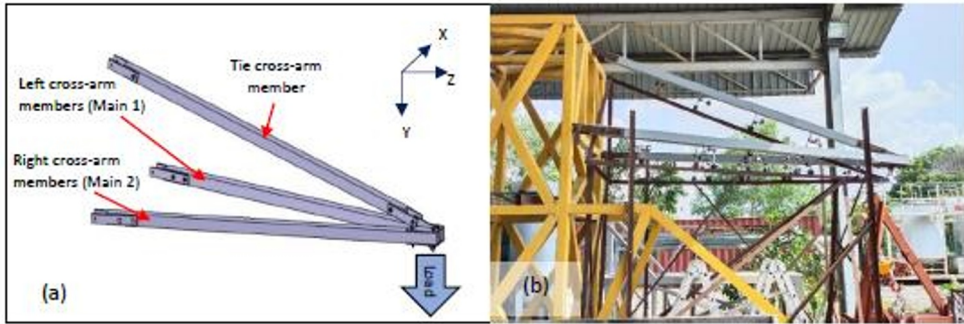


Fig. 1. The PGFRPC cross-arm assembly (a) schematic view (b) actual view

The current PGFRPC cross-arm was lay-up manually with a woven glass fiber method inspired by the hand lay-up method. The chosen location of the reinforcement was at the center of the main beam, which is the cross-arm beam's weakest point, as demonstrated by previous researchers. The length of the woven glass fiber lay-up was about 1.20 m. As the cross-arm did not have the common cylindrical shape, they were manually wrapped with woven glass fiber fabric using the lay-up method. The layers were carefully wrapped around the cross-arm as tight as possible as shown in Figure 2. Epoxy resin and hardener were mixed and applied to the layers on all four sides of the cross-arm with a roller.



Fig. 2. Complete assembled PGFRPC cross-arm (a) current cross-arm without improvement at the center of beam, (b) an improvement with manual woven glass fiber fabric wrapping method, (c) woven glass fiber fabric used in this research.

2.2 Methods of Research Activity

The properties of the improved PGFRPC cross-arm were investigated using a two-point bending test since the cross-arm application is the same as a cantilever beam. The testing methods were based on those developed by [4]. Dial gauges were used to determine the cross-arm deflection value and were positioned at five points (labeled as Y1 to Y5) on

each cross-arm member, as shown in Figure 3. Point Y1 was closest to the free end of the cross-arm and the gap between the gauges was set to 0.61 m. The applied load at the cross-arm free end was measured using a 3-ton crane scale. The load was gradually increased until the actual working load of 7.98 kN, as per the TNB standard, was achieved. Following that, the creep test was carried out for 1000 hours in the open area at the Aircraft Hangar, Faculty of Engineering, Universiti Putra Malaysia, in accordance with ASTM D2990. A static working load was hung at the free end of the PGFRPC cross-arm during the creep test, as shown in Figure 3 (b). Dial gauge deformation values were obtained at intervals of 0, 0.1, 0.2, 0.5, 1, 2, 5, 20, 50, 100, 200, 500, 700, and 1000 hours. The initial strain, often known as the "immediate strain," was measured 15 seconds after the working tension was applied. As the test was conducted in an open area, the cross-arms were exposed to the actual tropical weather and environmental conditions. The results of these tests would include the value of creep strain, modulus comparisons, and creep quantitative analysis on current and improved cross-arm designs.

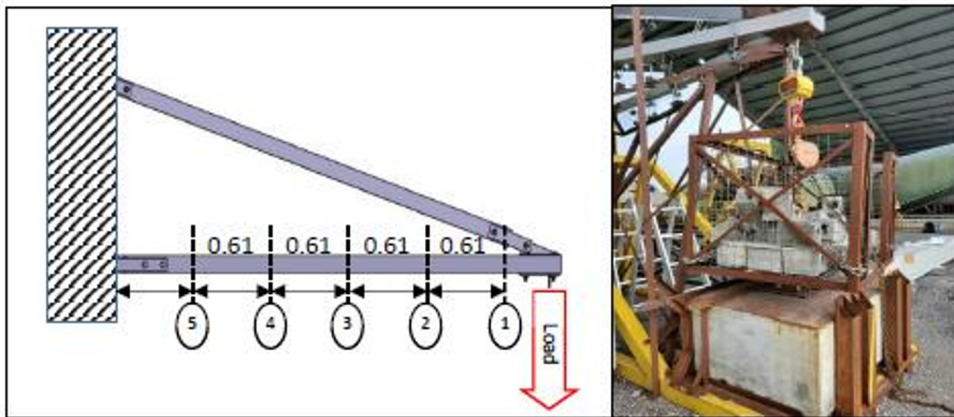


Fig. 3. PGFRPC cross-arm (a) dial gauge setup through the main beam (b) hanging static load arrangement during creep test.

The dial gauges were cleaned and lubricated with lubricant (DW40) to remove any rust or stains. In addition, a simple calibration was done using Mitutoyo analog dial gauge. These steps ensured that the gauges were in the best conditions for the tests. The dial gauges were then carefully aligned and placed on the points marked on both the left and right members of the cross-arm. Next, the dial gauges were turned on and reset to avoid zero errors during the measurement. On a side note, the dial gauges were preferred over the strain gauges because the latter were unsuitable for this experimental setup. The strain gauges were flat and adhered to the cross-arm members under the marked points Y1 to Y5. Over time, the strain gauges might detach themselves, eventually affecting the research results. Thus, dial gauges were deemed more suitable for this load deflection study and creep test.

2.3 Cross-Arms Creep Properties

A beam with a member that has one end projecting beyond the point of support should obey the cantilever beam concept. Because the cross-arm was horizontally extended from a fixed support, it was regarded as a cantilever beam structure for the purposes of this study. Therefore, the cross-arm mechanical properties were assessed using the cantilever beam equation and its derivations. The cross-arm members, where the upper section of the beam was in tension mode and the bottom section was in compressive mode, might be expected to deflect. The relationship between the force and deflection of the cantilever

beam was assumed to be linear as long as the deflection was small and the beam material did not yield. Since the cross-arm material used in this study was PGFRPC, thus it had a consistent density along its length. The basic principle of physics that mentioned by Hooke's Law said that the applied force or load is proportional to the extension y . Refer to Figure 4, the stress-strain relationship of the cross-arm can be defined as in Equation (1):

$$P = ky \quad (1)$$

Where P is the force exerted on the beam (N), k is the elastic coefficient (N/m) and y is the deflection (m). The elastic coefficient can be formulated based on Equation (2)

$$k = \frac{3E_e I}{L^3} \quad (2)$$

Where E_e is the Static Elastic Modulus (N/m²), I is the moment of inertia (m⁴) and L is the total cantilever beam length (m). By substitute Equation (1) into Equation (2), the elastic coefficient can be formulated as in Equation (3):

$$P = \left(\frac{3E_e I}{L^3} \right) \times y \quad (3)$$

By applied square shape moment of inertia formula for square cross-arm profile in Equation (3), the static elastic modulus (E_e) of cross-arm's beam can become as Equation (4):

$$E_e = \frac{4PL^3}{ybh^3} \quad (4)$$

Where the width and thickness dimensions of the cross-beam arm's (m) are b and h , respectively. Given that, the test results have previously revealed the y deflection. Thus, Equation (4) can be used to forecast the maximum bending stress. The cross-arm beam typically experiences its highest stress at the fixed point, $x=0$, and its minimum stress at the loading end, $x=L$. Equation (5) can be used to express the beam's maximum and minimum stresses (σ).

$$\sigma = \frac{P(L-x)\frac{h}{2}}{I} = \frac{6P(L-x)}{bh^2} \quad (5)$$

Equation (6) can be used to determine the strain across the beam at a certain time and place based on Hooke's Law.

$$\varepsilon_t = \frac{\sigma_n}{E_e} \quad (6)$$

Where ε_t is the strain across the cross-arm beam at a particular time and position, σ_n is the specific stress, and E_e is the static elastic modulus at that particular point on the cross-arm.

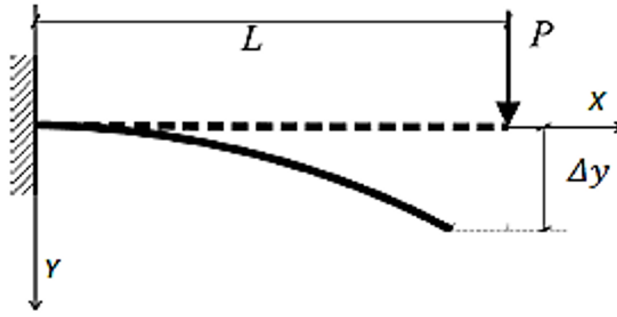


Fig. 4. Schematic diagram for a cross-arm structure which obey cantilever beam concept.

2.4 Empirical Creep Model

The study of creep properties of the PGFRPC cross-arm was further extended through the application of an established empirical creep model that was proven by previous researchers. This work used the nonlinear Findley power law model as an empirical model to support and explain transient creep in relation to the stress component and material constant. This model can be applied generically in every system, despite the fact that its application is constrained by the straightforward and direct numerical calculation in addition, the PGFRPC cross-arm was regarded as an isotropic substance. Thus, the Findley model was used to simulate the creep pattern and was represented by Equation.

$$\varepsilon_t = At^n + \varepsilon_0 \quad (7)$$

Where A and n are the time exponents and transient creep strain, respectively, and ε_0 is the instantaneous strain upon load exertion. Further discussion is presented in subsection 3.3 later.

3 Results and Discussion

This chapter presents and discusses the results of both load deflection and creep tests for the woven glass fiber fabric-reinforced cross-arms. This chapter also compares the creep-strain values as well as creep model for both the current cross-arm and the woven glass fiber fabric reinforced cross-arm. Finally, the adjusted regression ($Adj. R^2$) values of the Findley's model for current and wrapped cross-arm were also calculated and compared.

3.1 Load Deflection Behavior

The load-deflection values were measured using the dial gauges at all five points: Points Y1, Y2, Y3, Y4, and Y5. The cross-arms involved were those without woven glass fiber reinforcements and those reinforced with two, four, six, and eight layers of woven glass fiber. Each measurement was repeated thrice to obtain the average load deflection value. Then, the load-deflection values were plotted against the positions of the marked points: Y1 was the closest to the cross-arm free end while Y5 was the closest to the fixed point of the PGFRPC cross-arm

Figure 5 shows that the relationship between deflection behavior and load applied to the PGFRPC cross-arm was directly proportional. This relationship was valid as long as

the deflection was small, and the beam material did not yield. Thus, the PGFRPC is considered a linear elastic material that is homogeneous, isotropous and obeys Hooke's Law. The ultimate or maximum deflection was always at the free end, while the smallest deflection was at the cross-arm beam's fixpoint. The deflection behavior of this cross-arm was similar to that of the cantilever beam and covered a three-dimensional problem. The effect of Poisson's ratio can be ignored as the length of the beam was larger than the thickness of the perpendicular cross-section and shorter than the curvature radius of the beam.

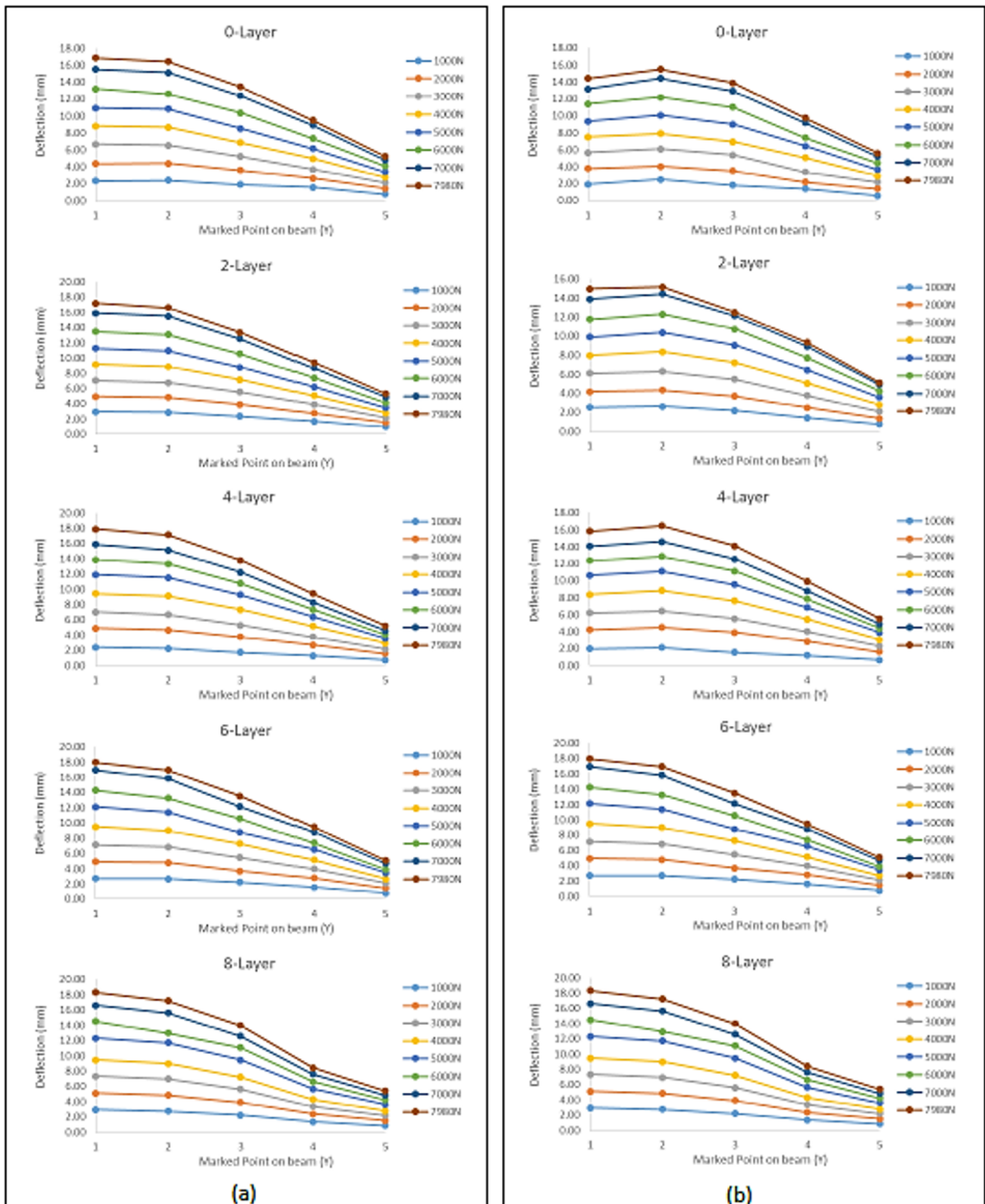


Fig. 5. The PGFRPC cross-arm load deflection results with and without woven fiber glass reinforcement (a) main 1 member, (b) main 2 member.

To study the effect of woven glass fiber reinforcement at the critical point (Point Y3), all cross-arm deflection values were used to investigate the beam behavior during the application of the working load. In the original state, namely without reinforcement, it was believed that the deflection of the right side of the cross-arm member was slightly smaller than the left side due to assembly fitting and fixed-point arrangement. As seen in Figure 5, the deflection values at Points Y4 and Y5 decreased as the number of woven glass fiber layers increased. It was observed that the deflection at Point Y3, wrapped with two layers of woven glass fiber, was smaller than that without reinforcement. This proves that reinforcing the cross-arm at its weakest point can improve the PGFRPC cross-arm strength.

Increasing the number of woven glass fiber layers further reduced the deflection value. However, only a slight improvement in cross-arm strength was observed. This might be due to the manual wrapping and layering process. The first two layers were tightly wrapped around Point Y3 without air bubbles or pockets. However, air pockets were observed after additional glass fiber layers were wrapped around Point Y3. This could be the main reason for the slight strength improvement. Thus, an automated woven glass fiber layering and wrapping process should be designed with a proper roller suitable for a square profile. The following sub-section presents the results of the investigation on the internal creep properties of reinforced PGFRPC cross-arm beams. In addition, a comparison between the results obtained in this work and by [4] was made and discussed.

3.2 Creep Strain Properties

Figure 6 illustrates the creep strain-time curves for the current and woven glass fiber-reinforced cross-arms under actual operating loads at Points Y1 to Y5. According to the effect of tension and compression along the main member beams during loading action, each strain gauge indicated a range of creep strain values. As the stress increased along the beam from the loading end to the fixed point, the elastic strain values changed along the length of the main member beams. This study demonstrates that the maximum creep strain was concentrated at Point Y3, which served as the centre of the current and reinforced cross-arm design's main members. Given that the working load was applied at the free end of the main member beams of the cross-arm structure, this result was attributed to beam buckling.

Comparing the results obtained from the original and reinforced PGFRPC cross-arms, it was observed that the creep strain on Main 1 and 2 was dissimilar due to unsymmetrically jig and fixing installation. However, their creep strain curve pattern was almost the same and followed the standard creep strain curves. This result is important as it shows that the cross-arm can withstand and sustain the loading conditions. This experimental arrangement was set up to mimic the real-world application and might have some

misalignment issues. Nevertheless, it was proven that the creep resistance performance of the cross-arm assembly could be improved by reinforcing the cross-arms with layers of glass fiber fabric. The cross-arm reinforced with eight layers of woven glass fiber experienced lower creep strain than the original cross-arm. This was due to the fabric interlayer contact mechanism, in which the lower layer overlapped the upper layer in the presence of epoxy resin, improving the beam's strength. Overall, reinforcement through the wrapping of composites reduced the buckling reaction and improved structural integrity.

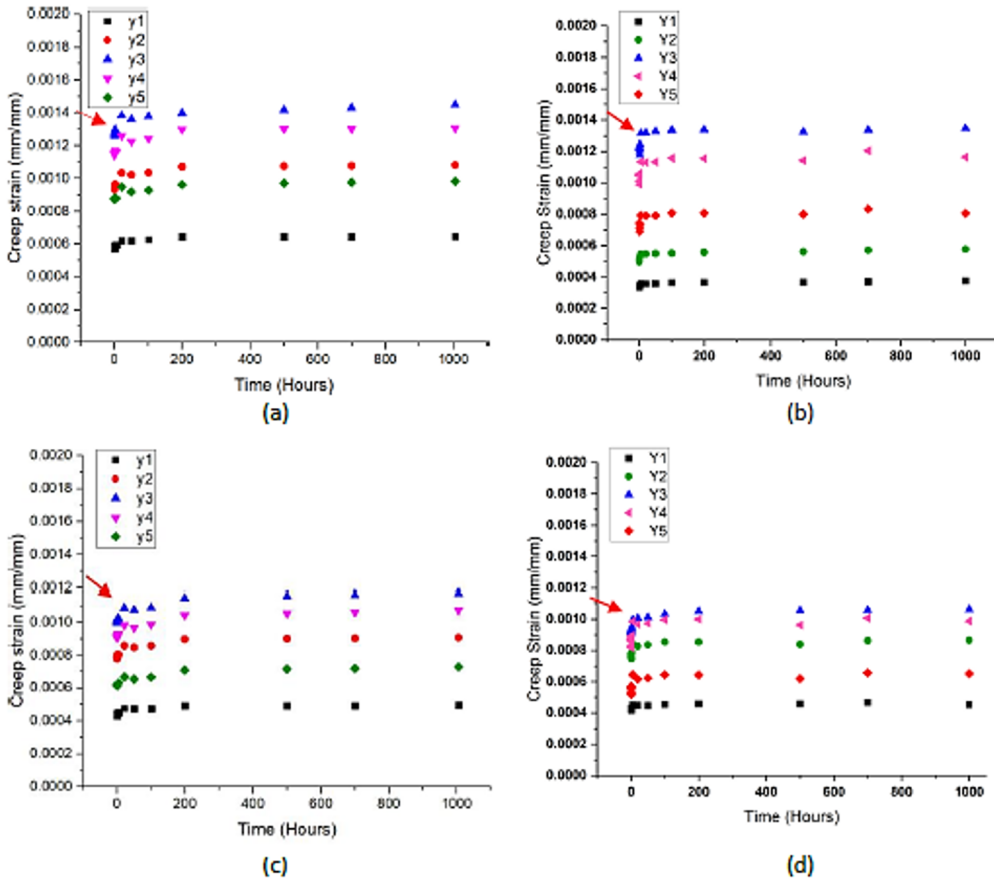


Fig. 6. The Creep strain-time curves for current PGFRPC cross-arm for (a) main 1 and (c) main 2; wrapped composite PGFRPC crossarm (b) main 1 and (d) main 2.

Figure 6(a) to (d) depicted creep strain patterns change from an elastic to a viscoelastic stage. The redarrows in Figure 6 illustrate how the creep strain curves of the original composite cross-arm showed an extended transition period from the elastic to the viscoelastic phase. The viscoelastic stage was efficiently reduced and made more stable by adding woven glass fibre to the structure, which decreased the possibility that the structure would fail. The strain value at Point Y3, which was larger in the current cross-arm than in the wrapped composite system, lends credence to this assertion. According to Figures 6 (a) and (b), the creep strain in the original Main 1 cross-arm exceeded 0.0014 mm/mm, while the creep strain in the reinforced cross-arm did not even reach 0.0014 mm/mm. For Main 2 cross-arm, the creep strain in the reinforced cross-arm was less than 10% of the current cross-arm. Overall, it can be said that to counter the lateral force from dead weight, which caused the structure to buckle, the creep resistance of the cross-arm assembly may be enhanced by adding greater composite layers.

3.3 Empirical Creep Model for PGFRPC Cross-Arm

The creep properties were analyzed by implementing an established creep model for cross-arm performance analysis, namely the Findley Power Law Model. The determined steady-

state creep of the cross- arm is shown in Table 1. The model was used to evaluate a number of parameters and is expressed by Equation (7). These variables included transient creep A and the material exponent n that is stress independent.

Table 1. The transient creep (A) and stress-independent material exponent (n) from Findley power law for current and wrapped PGFRPC cross-arm [22].

Main Cross-Arm Member	Location	A		n		$Adj. R^2$	
		Current Cross-Arm	Wrapped Cross-Arm	Current Cross-Arm	Wrapped Cross-Arm	Current Cross-Arm	Wrapped Cross-Arm
Main 1	1	3.207×10^{-4}	7.583×10^{-6}	0.021	0.224	0.961	0.989
	2	8.497×10^{-3}	4.393×10^{-3}	0.122	0.106	0.950	0.988
	3	5.602×10^{-3}	6.753×10^{-3}	0.195	0.142	0.959	0.990
	4	4.115×10^{-3}	4.637×10^{-3}	0.227	0.191	0.959	0.987
	5	2.663×10^{-3}	2.791×10^{-3}	0.232	0.189	0.951	0.988
Main 2	1	1.167×10^{-4}	1.431×10^{-3}	0.061	0.168	0.964	0.987
	2	1.506×10^{-4}	5.171×10^{-3}	0.088	0.139	0.942	0.988
	3	1.057×10^{-4}	6.729×10^{-3}	0.129	0.152	0.934	0.992
	4	1.183×10^{-4}	8.011×10^{-3}	0.119	0.130	0.903	0.989
	5	4.419×10^{-4}	4.053×10^{-3}	0.172	0.166	0.890	0.986

The transient creep A of the original and reinforced cross-arm listed in Table 1 were compared. It was observed that the reinforced cross-arm experienced a lower transient creep compared to the original composite cross-arm due to the superior steady-state creep response. This transient creep strain is the initial creep of inelastic flow, which decreases continuously until the steady state period is reached. The graph shows that glass fiber application did not influence the secondary creep stage because of the enhanced creep resistance of the PGFRPC cross-arm. The current composite cross-arm has a lower material stress independent exponent, n than the reinforced composite cross-arm, which was approximately 0.1366 and 0.1607, respectively (refer to Table 2). However, the n value for both original and reinforced cross-arms lay below the standard range of stress-independent material exponents of 0.20–0.29. Although improvements in load deflection results and transient creep value were observed in the reinforced composite cross-arm, a better composite wrapping method is required. In addition, the compatibility of woven glass fiber material needs to be further studied.

Table 2. Material stress independent exponent, n for current and wrapped cross-arms.

Configuration	Current Cross-Arm		Wrapped Cross-Arm	
	Main 1	Main 2	Main 1	Main 2
Material stress independent exponent, n	0.1594	0.1138	0.1704	0.1510
Average	0.1366		0.1607	

For the original and reinforced cross-arms, the adjusted regression ($Adj. R^2$) values of Findley's model were summarised in Table 1. The $Adj. R^2$ for the reinforced cross-arm ranged from 0.986 to 0.922. These numbers were quite near to 1, showing how effectively

Findley's model explained the experimental data. On the other hand, the *Adj. R²* values for the original cross-arm were in the range of 0.964 to 0.890. These findings demonstrate that the reinforced composite cross-arm adhered to the creep principle during the primary and secondary creep stages, and the creep data showed that increased structural integrity reduced exaggeration.

4 Conclusion

The purpose of this study was to evaluate the effect of adding woven glass fiber fabric as an additional reinforcement on the creep reactions of PGFRP composite cross-arms installed in a 132 kV transmission tower. Based on the results obtained from the experiments and the empirical study, the following conclusions can be drawn:

- The load-deflection for Main 1 and Main 2 does not really shows a gradually improved when compared with current cross-arm suspected due to glass fiber woven fabric wrapping process since it was done manually. In visual view, the first 2 layers were wrapped around the point Y3 nice and tight without any air bubbles or air pockets however the subsequent layers of 4, 6 and 8 had some air pockets unevenly.
- Although that, the creep strain patterns depicted a transitional phase from the elastic to the viscoelastic stage at all points and obviously shows decreasing almost 10% in the creep strain for wrapping cross-arm compared to current cross-arm at point Y3.
- The presence of wrapping glass-fiber woven fabric and reinforced with epoxy resin has improved the strength of weakest point at the PGFRPC cross-arm beam due to fabric interlayer contact mechanism on the glass fiber woven fabric of lower layer that are overlapping those the upper layer.
- By using the nonlinear Findley power law model, the wrapped cross-arm has shows lower transient creep value compared to current composite cross-arm design due to the superior steady-state creep response. However, the material stress independent exponent for both current and wrapped cross-arm lies below the common range as refer to previous study. Therefore the composite wrapped method need to be improve in fabrication method and the compatibility used of woven glass-fiber material.
- Several limitations that should be studied in the future such as the woven glass fiber fabric layup orientations, allowable slippage distance during overlapping states, dynamic results, flexibility reaction, failure mood, and creep analysis of the cross-arm structure during normal and broken wire conditions.

Considering these results and implications, this paper has highlighted the creep properties of current and improved PGFRPC cross-arm along with the possibility of further research in evaluate other mechanical properties. Research into this field is not developed as compared to other structures especially for PGFRPC material in high transmission tower application, and this gap must be narrowed in future works.

References

1. Amir, A.L.; Ishak, M.R.; Yidris, N.; Zuhri, M.Y.M.; Asyraf, M.R.M. Potential of honeycomb- filled composite structure in composite cross-arm component: A review

- on recent progress and its mechanical properties. *Polymers (Basel)*. **2021**, *13*, doi:10.3390/polym13081341.
2. Abdullah, N.; Hatta, N.M. Cloud-to-ground lightning occurrences in Peninsular Malaysia and its use in improvement of distribution line lightning performances. *PECon 2012 - 2012 IEEE Int. Conf. Power Energy* **2012**, 819–822, doi:10.1109/PECon.2012.6450330.
 3. Amir, A.L.; Ishak, M.R.; Yidris, N.; Zuhri, M.Y.M.; Asyraf, M.R.M. Advances of composite crossarms with incorporation of material core structures: Manufacturability, recent progress and views. *J. Mater. Res. Technol.* **2021**, *13*, 1115–1131, doi:10.1016/j.jmrt.2021.05.040.
 4. Asyraf, M.R.M.; Rafidah, M.; Ishak, M.R.; Sapuan, S.M.; Yidris, N.; Ilyas, R.A.; Razman, M.R. Integration of TRIZ, morphological chart and ANP method for development of FRP composite portable fire extinguisher. *Polym. Compos.* **2020**, *41*, 2917–2932, doi:10.1002/pc.25587.
 5. Liu, T.Q.; Liu, X.; Feng, P. A comprehensive review on mechanical properties of pultruded FRP composites subjected to long-term environmental effects. *Compos. Part B Eng.* **2020**, *191*, doi:10.1016/j.compositesb.2020.107958.
 6. Ozbakkaloglu, T.; Lim, J.C.; Vincent, T. FRP-confined concrete in circular sections: Review and assessment of stress-strain models. *Eng. Struct.* **2013**, *49*, 1068–1088, doi:10.1016/j.engstruct.2012.06.010.
 7. Zhang, Y.; Sun, L.; Li, L.; Huang, B.; Wang, T.; Wang, Y. Direct injection molding and mechanical properties of high strength steel/composite hybrids. *Compos. Struct.* **2019**, *210*, 70–81, doi:10.1016/j.compstruct.2018.11.035.
 8. Forintos, N.; Czigany, T. Multifunctional application of carbon fiber reinforced polymer composites: Electrical properties of the reinforcing carbon fibers – A short review. *Compos. Part B Eng.* **2019**, *162*, 331–343, doi:10.1016/j.compositesb.2018.10.098.
 9. Mohamad, D.; Syamsir, A.; Beddu, S.; Abas, A.; Ng, F.C.; Razali, M.F.; Seman, S.A.H.A. Numerical Study of Composite Fiberglass Cross Arms under Statics Loading and Improvement with Sleeve Installation. In Proceedings of the IOP Conference Series: Materials Science and Engineering; 2019; Vol. 530.
 10. Mohamad, D.; Beddu, S.; Syamsir, A.; Zahari, N.M.; Razali, M.F.; Abu Seman, S.A.H.; Abas, A.; Ng, F.C. Failure analysis of various fiberglass cross-arm designs under multi-axial loading. In Proceedings of the IOP Conference Series: Materials Science and Engineering; 2020; Vol. 920.
 11. S.A.H.A. Numerical Simulation on the Statics Deformation Study of Composite Cross Arms of Different Materials and Configurations. In Proceedings of the IOP Conference Series: Materials Science and Engineering; 2019; Vol. 530.
 12. Ang, J.Y.; Abdul Majid, M.S.; Mohd Nor, A.; Yaacob, S.; Ridzuan, M.J.M. First-ply failure prediction of glass/epoxy composite pipes using an artificial neural network model. *Compos. Struct.* **2018**, *200*, 579–588, doi:10.1016/j.compstruct.2018.05.139.
 13. Mohamad, D.; Syamsir, A.; Sa'Don, S.N.; Zahari, N.M.; Seman, S.A.H.A.; Razali, M.F.; Abas, A.; Ng, F.C. Stacking Sequence Effects on Performance of Composite Laminate Structure Subjected to Multi-Axial Quasi-Static Loading. In Proceedings of the IOP Conference Series: Materials Science and Engineering; 2019; Vol. 530.
 14. Mohamad, D.; Syamsir, A.; Beddu, S.; Kamal, N.L.M.; Zainoodin, M.M.; Razali, M.F.; Abas, A.; Seman, S.A.H.A.; Ng, F.C. Effect of Laminate Properties on the Failure of Cross Arm Structure under Multi-Axial Load. In Proceedings of the IOP Conference Series: Materials Science and Engineering; 2019; Vol. 530.

15. Russell, B.P.; Deshpande, V.S.; Wadley, H.N.G. Quasistatic deformation and failure modes of composite square honeycombs. *J. Mech. Mater. Struct.* **2008**, *3*, 1315–1340, doi:10.2140/jomms.2008.3.1315.
16. Singhal, D.; Narayanamurthy, V. Large and Small Deflection Analysis of a Cantilever Beam. *J. Inst. Eng. Ser. A* **2019**, *100*, 83–96, doi:10.1007/s40030-018-0342-3.
17. Nallathambi, A.K.; Lakshmana Rao, C.; Srinivasan, S.M. Large deflection of constant curvature cantilever beam under follower load. *Int. J. Mech. Sci.* **2010**, *52*, 440–445, doi:10.1016/j.ijmecsci.2009.11.004.
18. Zeng, W.; Yan, J.; Hong, Y.; Cheng, S.S. Numerical analysis of large deflection of the cantilever beam subjected to a force pointing at a fixed point. *Appl. Math. Model.* **2021**, *92*, 719–730, doi:10.1016/j.apm.2020.11.023.
19. Wang, T.M. Nonlinear bending of beams with concentrated loads. *J. Franklin Inst.* **1968**, 285, 386–390, doi:10.1016/0016-0032(68)90486-9.
20. Tari, H. On the parametric large deflection study of Euler-Bernoulli cantilever beams subjected to combined tip point loading. *Int. J. Non. Linear. Mech.* **2013**, *49*, 90–99, doi:10.1016/j.ijnonlinmec.2012.09.004.
21. Beléndez, T.; Neipp, C.; Beléndez, A. Numerical and Experimental Analysis of a Cantilever Beam: A Laboratory Project to Introduce Geometric Nonlinearity in Mechanics of Materials. *Int. J. Eng. Educ.* **2003**, *19*, 885–892.
22. Aniskevich, K.; Aniskevich, A.; Arnautov, A.; Jansons, J. Mechanical properties of pultruded glass fiber-reinforced plastic after moistening. *Compos. Struct.* **2012**, *94*, 2914–2919, doi:10.1016/j.compstruct.2012.04.030.
23. Shindo, Y.; Takeda, T.; Narita, F.; Saito, N.; Watanabe, S.; Sanada, K. Delamination growth mechanisms in woven glass fiber reinforced polymer composites under Mode II fatigue loading at cryogenic temperatures. *Compos. Sci. Technol.* **2009**, *69*, 1904–1911, doi:10.1016/j.compscitech.2009.04.010.
24. Fu, H.; Dun, M.; Wang, H.; Wang, W.; Ou, R.; Wang, Y.; Liu, T.; Wang, Q. Creep response of wood flour-high-density polyethylene/laminated veneer lumber coextruded composites. *Constr. Build. Mater.* **2020**, *237*, doi:10.1016/j.conbuildmat.2019.117499.
25. Asyraf, M.R.M.; Ishak, M.R.; Sapuan, S.M.; Yidris, N.; Shahroze, R.M.; Johari, A.N.; Rafidah, M.; Ilyas, R.A. Creep test rig for cantilever beam: fundamentals, prospects and present views. *J. Mech. Eng. Sci.* **2020**, *14*, 6869–6887, doi:10.15282/jmes.14.2.2020.26.0538.
26. Beléndez, T.; Neipp, C.; Beléndez, A. Large and small deflections of a cantilever beam. *Eur. J. Phys.* **2002**, *23*, 371–379, doi:10.1088/0143-0807/23/3/317.
27. Mohamad, D.; Beddu, S.; Syamsir, A.; Zahari, N.M.; Abu Seman, S.A.H.; Razali, M.F.; Abas, A.; Ng, F.C. Performance Evaluation of Composite Cross-Arm Structure under Different Magnitude of Loading. In Proceedings of the IOP Conference Series: Materials Science and Engineering; 2020; Vol. 920.
28. Feynman, R.P. Feynman lectures on physics. Volume 2: Mainly electromagnetism and matter. In *American Journal of Physics*; Addison-Wesley Pub (Sd), 1964; Vol. 33, p. 750 ISBN 9780201020113.